DYNAMIC RESPONSE OF R/C COOLING TOWER SHELL CONSIDERING SUPPORTING SYSTEMS

Takashi HARA

Tokuyama College of Technology

ABSTRACT: R/C cooling towers are used for many kinds of industrial and power plants. These are huge structures and also show thin shell structures. R/C cooling towers are subjected to its self-weight and the dynamic load such as an earthquake motion and a wind effects. Especially, dynamic analyses of these structures are important factor to design R/C cooling tower structures. In this paper, dynamic behavior of R/C cooling tower shell under an earthquake loading is analyzed by use of FEM focused on the column arrangement systems. To reduce the computational efforts to solve such problems, the technique for a parallel computing is applied. To solve the nonlinear dynamic response of a huge cooling tower with local deviation, the element by element (EBE) parallel approach is adopted by using of PC cluster. From the numerical analyses, the effects of the combination of R/C shell and column systems are examined.

1. INTRODUCTION

R/C cooling towers are used for many kinds of industrial and power plants. These are huge structures and also show thin shell structures. R/C cooling towers are subjected to its self-weight and the dynamic load such as an earthquake motion and a wind effects. Especially, dynamic analyses of these structures are important factor to design R/C cooling tower structures constructed around the region of a frequent earthquake. However, it is difficult to solve these problems because R/C structure composes of a concrete and reinforcements and both materials show nonlinear behavior. In particular, nonlinear behavior of concrete is complicate to represent mathematically.

A quasi-static loading is applied to design R/C cooling tower instead of dynamic response analysis because of the difficulty of representing the dynamic material properties. In addition, these structures have huge surfaces of concrete with increasing its constructional height and also, R/C shell structure is usually placed on the supporting columns to take a cold air into it. R/C cooling tower represents the combinations of R/C shell and R/C column structures. Consequently, the huge R/C shell structural behavior with local deviations must be solved.

To solve such problems, many numerical schemes have been proposed combining the axisymmetric analyses or modal analyses [Hara et.al 2002, Lang et. al. 2003]. However, it is difficult to represent the local behavior of these structures by such numerical scheme. To overcome these problems, the finite element method (FEM) is one of the useful schemes. On the other hand, to apply FEM to such problems, there must be a numerical effort to solve these structures under a dynamic loading.

In this paper, dynamic behavior of R/C cooling tower shell under a earthquake loading is analyzed by use of FEM focused on the column arrangements and column systems. To reduce the computational efforts to solve such problems, the technique for a

parallel computing is applied. To solve the nonlinear dynamic response of a huge cooling tower with local deviation, the element by element (EBE) parallel approach is adopted by using of PC cluster. The efficiencies of applying EBE parallel algorithms to R/C structures were discussed (Hara et. al. 2004 and Hara 2005).

From the numerical analyses, the nonlinear dynamic response of R/C cooling tower is examined and the effects of the combination of the shell and column structural systems are examined.

2. FEM PROCEDURE

2.1 Finite Element

In order to investigate the failure mechanisms of R/C cooling tower under dynamic loading, a finite element procedure is adopted. In this analysis, the isoparametric hexahedral element with 20 nodes is adopted. Each node has three translation degrees of freedom. To evaluate the volumetric integration, 15 points selective integration is adopted (Hinton 1988). R/C cooling tower is divided into such three dimensional elements.

2.2 Material Properties of Concrete

Reinforced concrete is composed of concrete and reinforcements. To represent the concrete material, it is assumed that the concrete behaves as linear material before stresses do not exceed the yield stress defined by the yield function. After yielding of the material, the inelastic behavior of concrete is assumed to possess the recoverable and irrecoverable strain components.

Under triaxial stress state, the yield function depends not only on the mean normal stress I_1 but also on the second deviatoric stress invariant J_2. The yield condition of triaxial compressive concrete is expressed as follows:

$$f(I_1, J_2) = \sqrt{\beta(3J_2) + \alpha I_1} = \sigma_0 \qquad (1)$$

where α and β are material parameters. Referring to Eq. (1) the three dimensional stress states and the yield functions are shown in Figure 1. When the two dimensional experimental results reported by Kupfur's (Kupher 1966) are employed, $\alpha=0.355\ \alpha_0$ and $\beta=1.355$ are defined. Also, in Eq.(1), σ_0 is the equivalent effective stress.

To define the hardening rule, the relationship between the accumulated plastic strain and the current 'loading surface' (Figure 1) is assumed to be conventional 'Madrid Parabola' (Figure 2) (Hinton 1988)

$$\sigma = E_0 \varepsilon - \frac{1}{2}\frac{E_0}{\varepsilon_0}\varepsilon^2 \qquad (2)$$

where E_0 and ε_0 represent the initial elastic modulus and the total strain at peak stress, respectively.

It is assumed that the initial yield begins when the equivalent stress exceeds $0.3f_c$ (f_c: compressive strength of concrete)
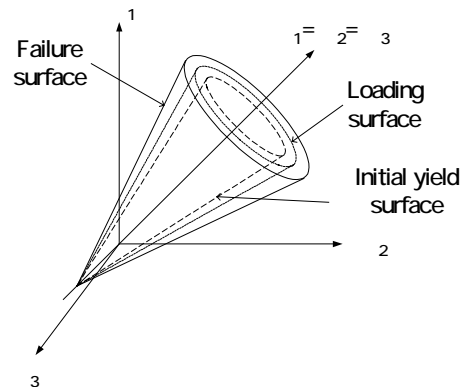
Figure 1 Concrete in compression
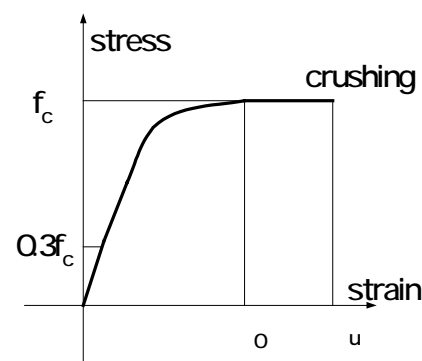
Figure 2 Madrid Parabola

The crushing condition of concrete is described as a strain control phenomenon and the crushing condition is defined as like as the yield condition in Eq. (1).

The response of concrete in tension is modeled as a linear-elastic brittle material and maximum tensile stress criteria are employed. Three dimensional stress space representations in tension-compression status are shown in Figure 3.
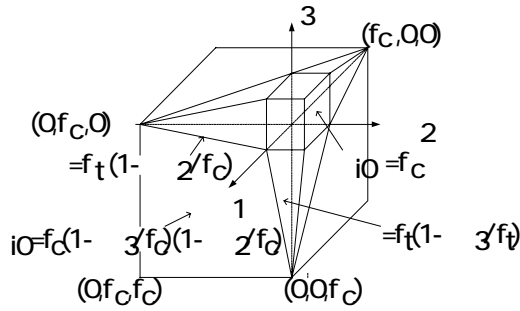
Figure 3 Crack condition

After cracking, to evaluate the tension stiffening of reinforced concrete, the stress reduction of the concrete normal to the cracked plane is assumed as shown in Figure 4.
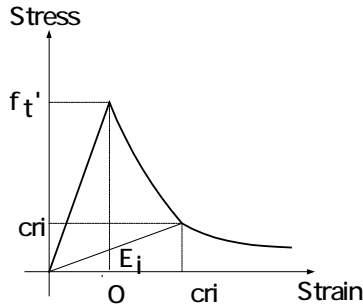
Figure 4 Concrete in Tension

In Figure 4, the stress in degradation zone is defined as follows.

$$\sigma = f_t' \exp\left(-\frac{\varepsilon - \varepsilon_t'}{\gamma}\right) \qquad \gamma = \frac{G_f - 0.5 f_t' \varepsilon_{cr}\ell_c}{f_t\ell_c} \qquad (3)$$

where f_t' is maximum tensile strength of concrete, γ is the tension stiffing parameter, ε_i' is crack strain, G_f is the fracture energy of concrete, ℓ_c is the cubic root of volume in Gaussian point and ε_{cr} is the strain in crack. $\gamma = 0.2$ is adopted in this paper.

When the strain reversal appears, the relation between the stress and the strain is defined using the modulus E_i.

2.3 Material Properties of Reinforcements

The reinforcing bars are considered as steel sheets that possess equivalent thickness and has uniaxial behavior resisting only against the axial force in the bar direction (see Figure 5). The bilinear idealization is adopted in order to model the elasto-plastic stress strain relationship and both the tensile and the compressive state are governed by the same relationship. These steel layers are assigned into each shell element.

The material properties of concrete and reinforcements are shown in Table 1.
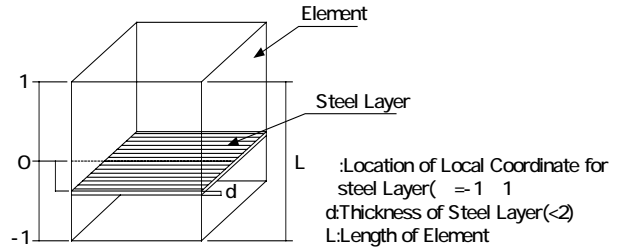
Figure 5 Local coordinate and location of steel layer

Table 1 Material Properties

Concrete	
Elastic Modulus	34Gpa
Poisson's Ratio	0.167
Density	0.0023kg/cm^3
Compressive Strength	36MPa
Tensile Strength	2.7MPa
Reinforcement	
Elastic Modulus	206GPa
Tangent Modulus	2.1GPa
Yield Stress	500MPa

2.4 Dynamic Analyses

For each element, the element stiffness **k** and the element mass matrices **m** are defined under the assumption mentioned above. Assembling these matrices, the dynamic equilibrium equations are derived. During the time increment, the dynamic equilibrium equation is represented as follows:

$$\mathbf{M}\Delta\ddot{\mathbf{y}} + \mathbf{C}\Delta\dot{\mathbf{y}} + \mathbf{K}\Delta\mathbf{y} = -\mathbf{M}\mathbf{I}\Delta\ddot{\mathbf{y}}_0 \qquad (4)$$

where $\mathbf{M}$ is the mass matrix, $\mathbf{C}$ is the damping matrix, $\mathbf{K}$ is the stiffness matrix. $\Delta\mathbf{y}$, $\Delta\dot{\mathbf{y}}$ and $\Delta\ddot{\mathbf{y}}$ are the response displacement, the response velocity and the response acceleration vector, respectively. $\Delta\ddot{\mathbf{y}}_0$ is the ground motion acceleration and Δ denotes the incremente. In this analysis, Raileigh damping is adopted to define the damping matrix.

$$\mathbf{C} = a_1\mathbf{M} + a_2\mathbf{K} \qquad (5)$$

where a_1 and a_2 are the constants.

To solve Eq.(4), the Newmark method is adopted in this paper. Then, substituting the Newmark representations of the velocity and the acceleration vector into the dynamic equiliburium equation systems, Eq. (4) is transformed as follows:

$$\tilde{\mathbf{K}}\mathbf{y} = \tilde{\mathbf{f}} \qquad (6)$$

where

$$\tilde{\mathbf{K}} = \frac{\mathbf{M}}{\beta\Delta t^2} + \frac{\mathbf{C}}{2\beta\Delta t} + \mathbf{K} \qquad (7)$$

and

$$\tilde{\mathbf{f}} = -\mathbf{M}\mathbf{I}\Delta\ddot{\mathbf{y}}_0 + \mathbf{M}\left(\frac{\Delta\dot{\mathbf{y}}}{\beta\Delta t} + \frac{\Delta\ddot{\mathbf{y}}}{2\beta}\right) +$$
$$+ \mathbf{C}\left\{\frac{\Delta\dot{\mathbf{y}}}{2\beta} + \left(\frac{1}{4\beta} - 1\right)\Delta\ddot{\mathbf{y}}\Delta t\right\} \qquad (8)$$

are the effective stiffness matrix and the mofdified load vectors, respectively.

In this paper, the dynamic response is evaluated with a time step of $\Delta t = 0.001$sec. The damping facter is considered 3% proportial to the mass by Rayleigh damping (Eq.(5)). The convergence rule of equation of motion is defined by Newton-Raphson method.

2.5 EBE Procedure

In the dynamic response of structure, Eq. (6) is solved step by step. However, to solve this equation, we need a large computing effort because R/C cooling tower model possesses large amount of degrees of freedom. Although, to solve such problems, many numerical schemes have been proposed combining the axisymmetric analyses or modal analyses, it is also difficult to represent the local behavior of these structures by such numerical scheme. To overcome these problem, a parallel computation is one of the solution schemes to solve such large size of simultaneous equations. In these analyses, element-by-element (EBE) solution techniques (Hughes 1983, Levit 1987, Hara 2004) are applied to Eq.(6).

Each term of Eq.(6) is assembled by each element equilibrium equations. Then the equation is solved by use of the conjugate gradient method (Adeli 1999).

PC cluster is applied to solve Eq. (6). In this analysis, PC cluster is composed of 8 personal computers and a switching hub to connect each other. The data communication of each computer is governed by MPI.

In conjugate gradient scheme, the solution vector $\mathbf{y}_{k+1}$ and the gradient vector $\mathbf{r}_{k+1}$ are represented as follows:

$$\mathbf{y}_{k+1} = \mathbf{y}_k - \alpha_k\mathbf{p}_k \qquad (9)$$

$$\mathbf{r}_{k+1} = \mathbf{r}_k - \alpha_k\tilde{\mathbf{K}}\mathbf{p}_k \qquad (10)$$

where

$$\alpha_k = \frac{\mathbf{r}_k^T\mathbf{r}_k}{\mathbf{p}_k^T\tilde{\mathbf{K}}\mathbf{p}_k} \qquad (11)$$

and

$$\mathbf{p}_{k+1} = \mathbf{r}_k + \beta_{k+1}\mathbf{p}_k \qquad (12)$$

$$\beta_{k+1} = \frac{\mathbf{r}_{k+1}^T\mathbf{r}_{k+1}}{\mathbf{r}_k^T\mathbf{r}_k} \qquad (13)$$

In Eqs. (9)-(13), $\tilde{\mathbf{K}}\mathbf{p}_k$ is calculated by element by element. Therefore, these are easy to parallelized.

To define the vector $\mathbf{r}_0$, the preconditioning technique is usually adopted. In this analysis, the solutions are relatively stable and the iterative solution converges well. Therefore, the preconditioning of the equation is not adopted to solving Eq. (6) by the conjugate gradient scheme.

3 NUMERICAL MODEL

Applying the parallel computing scheme mentioned above to R/C cooling tower, the dynamic response of structure is analyzed.

3.1 Geometry of R/C cooling tower

The geometric configuration R/C shell is defined as follows (Hara 2004):

$$r = \Delta r + a \cdot \sqrt{1 + \frac{(z-125)^2}{b^2}} \qquad (14)$$

where r is the radius of the shell at height z(m). Parameters a, b and Δr are shown in Table 2. Also, the radius and the thickness of R/C shell are presented in Table 3.

3.2 Reinforcements

In shell elements, reinforcements are placed in both hoop and meridional directions on both inner and outer surface of the shell. The reinforcing ratio of each reinforcing layer is assumed to be 0.2%.

Table 2. Configuration parameters

Height(z)	9.17m-125m	125m-176m
a	51.9644	0.2578
b	113.9896	8.0293
Δr	-15.3644	36.3422

Table 3. Radius and thickness of the shell

	Lintel	Node	Top
Height(z)	9.17m	125m	176m
Radius(m)	58.72m	36.6m	38.0m
Thickness(m)	1.05m	0.24m	0.2m

The concrete covers are 15% thickness of the shell wall from both inner and outer surfaces. The material properties of the concrete and the reinforcements are shown in Table 1.

3.3 Analytical Model

Figure 6 shows the numerical models of the R/C cooling tower. The model is a half of R/C shell considering the symmetry of the configuration, the loading and supporting conditions. Both models are divided into 32 elements in hoop direction and into 30 elements in meridional direction. The height is about 175m. The thickness of the shell changes 105cm at the lintel through 20cm at the top (see Table 3). In R/C shell structure, reinforcements are doubly placed in both hoop and meridional direction. The reinforcing ratio is 0.2%. On the other hand, reinforcements are placed 2% in the columns. R/C hyperbolic shell is supported on the 16 columns. Each column has 90cm square cross section and 9.17m length. In I column model, the supporting columns are placed equidistance. In V column model, the supporting columns are placed equidistance and the adjacent top of the columns are connected. Each column is divided into four elements to represent the flexural deformation of the columns.
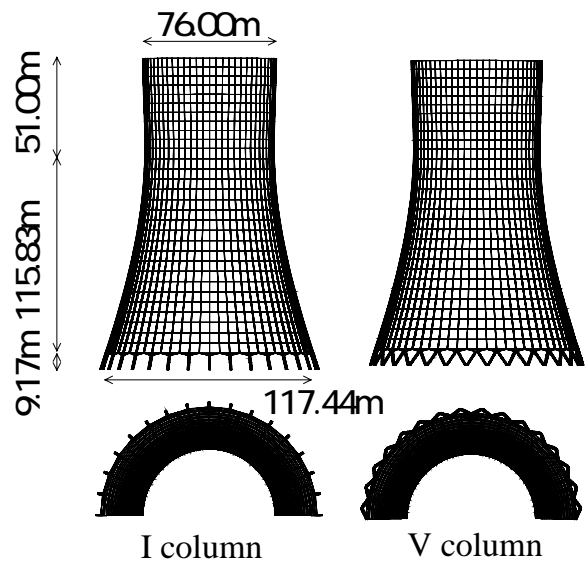
I column   V column

Figure 6 numerical Models

4 NUMERICAL RESULTS

To compare the dynamic characteristics of the shell with two types of columns, the step load and the harmonic loads are applied to the models.

displacement(cm)
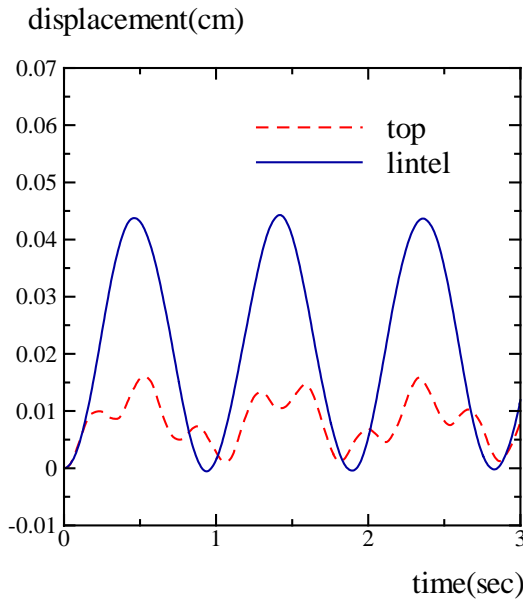
Figure 7 Response of Step Load (I-Column)

displacement(cm)
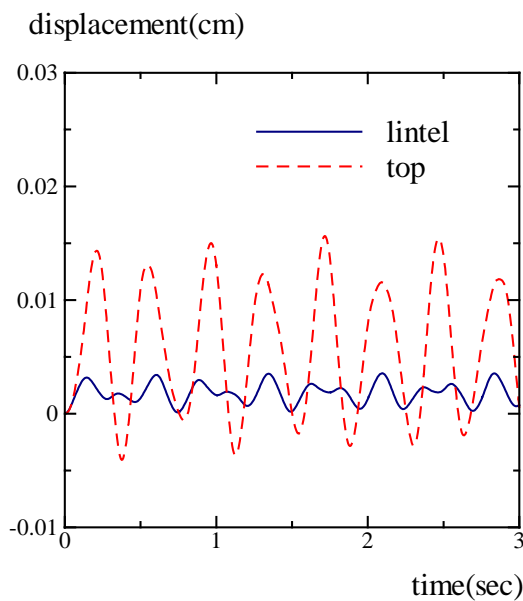
Figure 8 Response of Step Load (V-Column)

4.1 R/C Cooling Tower under Step Loading

To evaluate the basic dynamic response properties of R/C cooling tower, the step load of 0.1g (g: gravity acceleration 980cm/s^2) is applied. Figures 7 and 8 show the time displacement history at the top (the dash line) and at the lintel (the solid line) of the shell under the step load. These figures represent the responses for the shell with I-columns and with V-columns, respectively.

In the shell with I-columns, the response at the lintel is larger than that at the top, while the response at the lintel is smaller than that at the top in the shell with V-columns. From these responses, the shell with V-columns shows the small displacements and is stiff enough against the lateral load.

From Figure 7, the natural frequency of the shell with I-columns is 1.05Hz. Also, Figure 7 shows the 2.70Hz from the top response. In the case of the shell without columns, the natural frequency of this model shows 3.5Hz (Hara 2004).

From Figure 8, the natural frequency of the shell with V-columns is 2.66Hz. The amplitudes of the displacements on both lintel and the top are different. But the natural frequencies of them are the same.

Figures 9 and 10 show the deformation patterns of R/C cooling tower with I-columns and V-columns, respectively. The deformation of the shell with I-column represents the kink at the connection between the shell and the columns and the shell shows the rigid body rotation. On the other hand, the response of R/C cooling tower with V-column deforms like as the cantilevered column.
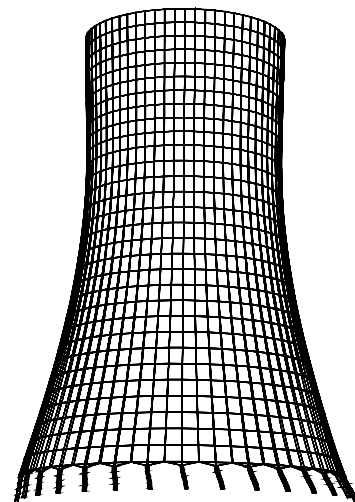
Figure 9 Deformation under Step Load
(I-column)
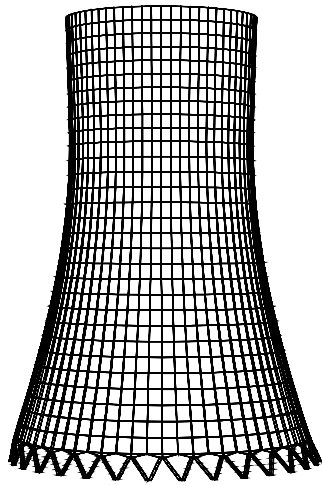
Figure 10 Deformation under Step Load

(V-column)

4.2 R/C Cooling Tower under Harmonic Loading

Figures 11 and 12 show the responses of the cooling tower with I-columns and V-columns under the harmonic loading, respectively. The dotted and the solid line denote the response at the top and the lintel, respectively. In this analysis, the intensity of the load is 0.1g.

The frequencies of an external harmonic load are 1.05Hz for the shell with I-columns and 2.66Hz for the shell with V-columns, respectively.
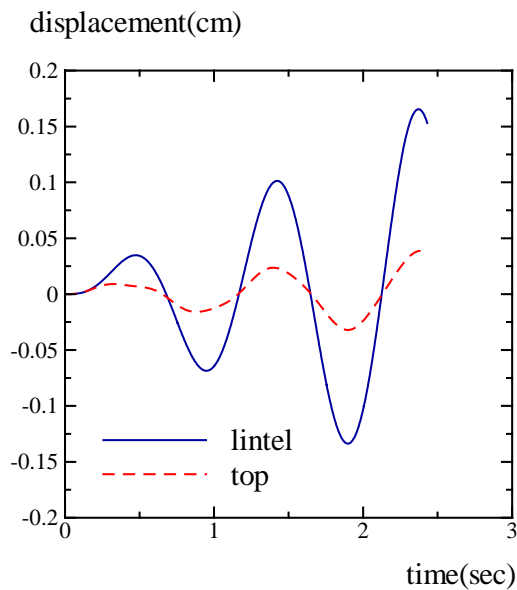
Figure 11 Response under Harmonic loading

(I-column)
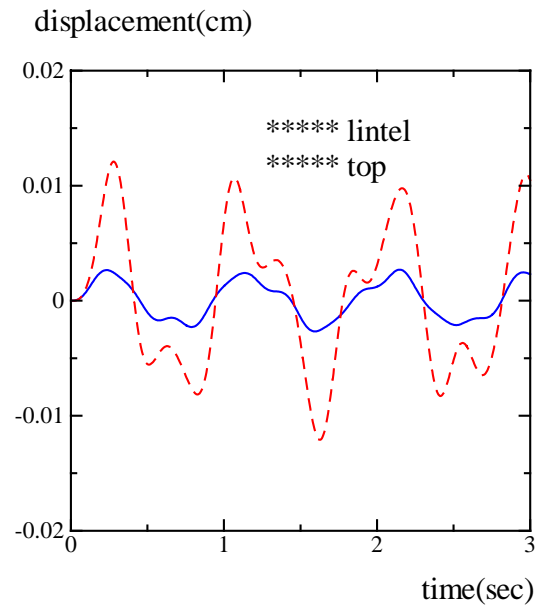
Figure 12 Response under Harmonic loading

(V-column)

Each frequency of the harmonic load is adopted considering their natural frequency under step loadings.

Figure 11 shows the resonance response of the structure. In the case of I-columns, the large deformation is detected around the conjunction between the lintel and columns.

Figure 12 does not show the resonance response of the structure within 3 seconds. The cooling tower shell with V-columns shows the same deformation mode as that shown under step loading.

5 CONCLUSIONS

This paper presented the numerical analysis of R/C cooling tower with column support under dynamic loading. To apply the general finite element to solve the huge R/C structure, the parallel computing technique is adopted.

In numerical analyses, two types of the supporting column systems are adopted and the the dynamic response of R/C cooling tower is examined. Also, the EBE approach to the huge R/C structures is applied.

From the numerical investigations, following conclusions are obtained.

(1) R/C cooling tower with I-column supports under dynamic loading shows local deformation around the junction between the lintel and columns but shows small deformation or distortion on the shell.

(2) R/C cooling tower with V-column supports under dynamic loading shows the cantilever type global deformation but the deformation is small.

(3) The total structural responses of the shell with supporting columns strongly depend on the column supporting systems and are different from the conventional pin-supported ideal shell (Hara 2004). Therefore, the precise total analyses must be considered.

The numerical scheme presented here will be applicable to the practical one such as the earthquake response of the structure or the response of the dynamic wind loading considering the local deviations such as supporting columns and the hole on the shell surface.

REFERENCES

Adeli H. and Soegiarso R., 1999, *High-performance computing in structural engineering*. CRC Press

Hara T. and Gould P.L., 2002, Local-global analysis of cooling tower with cutout*s*, *Computers & Structures,* **80**:2157-2166.

Hara T., 2004, Dynamic analysis of R/C cooling tower shells under earthquake loading. *5th International Symposium on Natural-Draught Cooling Towers.* 283-291

Hara T., 2004, Dynamic response analysis of R/C cooling tower shell, *Proceedings of the WCCM VI in conjunction with APCOM'04, Sep. 5-10, 2004, Beijing, China* on CDROM.

Hara T. and Hadi M.N.S., 2005, Behavior of eccentrically loaded concrete columns with FRP wrapping, Proceedings of ISEC-03, Sep.20-23, Shunan, Japan, **1**:229-235.

Hinton E., 1988, *Numerical methods and software for dynamic analysis of plates and shells*. Pineridge press Swansea U.K.

Hughes T.J.R, Levit I. and Winget J., 1983, An element-by-element solution algorithm for problems of structural and solid mechanics. *Computer Methods in Applied Mechanics and Engineering* **36**:241-254

Kupfer H. and Hilsdorf K.H., 1966, Behavior of concrete under biaxial stress., *ACI Journal* **66**:656-666.

Lang C., Meiswinkel R. And Wittek U., 2003, Anwendung von Schalenringelementen zur nichtlinearren dynamischen Berechnung von Stahlbeton- Rotationsschalen, *Beton- und Stahlbetonbau*, **98**:123-134, (in German).

Levit I., 1987, Element-by-element solvers of order N. *Computers & Structures* **27**:357-360